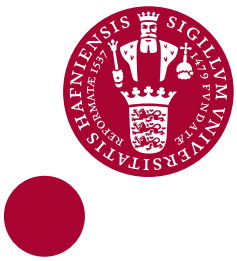

Vertical Migration Optimizes Photosynthetic Efficiency of Motile Cyanobacteria in a Coastal Microbial Mat

Lichtenberg, Mads; Cartaxana, Paulo; Kühl, Michael

Published in:
Frontiers in Marine Science

DOI:
10.3389/fmars.2020.00359

Publication date:
2020

Document version
Publisher's PDF, also known as Version of record

frontiers in Marine Science

ORIGINAL RESEARCH
published: 25 May 2020
doi: 10.3389/fmars.2020.00359

Vertical Migration Optimizes Photosynthetic Efficiency of Motile Cyanobacteria in a Coastal Microbial Mat

*Mads Lichtenberg†, Paulo Cartaxana† and Michael Kühl**

Marine Biological Section, Department of Biology, University of Copenhagen, Copenhagen, Denmark

Microbial mats are diverse and stratified microbial biofilm communities characterized by steep gradients in light, temperature and chemical parameters. Their high optical density creates a competition for light among phototrophic microalgae and bacteria residing in the uppermost mat layers. Strategies to counter such resource limitation include metabolic investment in protective and light-harvesting pigments enabling exploitation of separate niches in terms of irradiance and spectral composition, or investment in motility to enable migration to an optimal light microenvironment. We used microsensor measurements of light, temperature and gross photosynthesis in coastal microbial mats dominated by motile cyanobacteria and colorless sulfur bacteria to study how migration affected their radiative energy-budgets and relative photosynthetic efficiency. The optical density of the microbial mat was extremely high, and >99% of incident irradiance of visible light (400–700 nm) was attenuated <0.4 mm below the surface. While energy conservation efficiency did not change dramatically with previous light acclimation, vertical profiles of photosynthetic efficiency showed a shift in the position of maximum efficiency of ∼0.2 mm, depending on light treatment. Besides avoidance of unfavorable chemical conditions such as high sulfide levels, vertical migration over short distances thus enable cyanobacteria to track zones with optimal light exposure thereby efficiently counteracting detrimental effects of excessive light at the surface and insufficient light deeper in the mat.

Keywords: biofilm, light, microenvironment, microsensors, photosynthesis, cyanobacteria

OPEN ACCESS

Edited by:
Vona Meleder, Université de Nantes, France

Reviewed by:
Bo Barker Jørgensen, Aarhus University, Denmark
Dirk de Beer, Max-Planck-Gesellschaft (MPG), Germany

***Correspondence:**
Michael Kühl
mkuhl@bio.ku.dk

†Present address:
Mads Lichtenberg, Costerton Biofilm Center, University of Copenhagen, Copenhagen, Denmark
Paulo Cartaxana, Departamento de Biologia & CESAM & ECOMARE, Universidade de Aveiro, Aveiro, Portugal

Specialty section:
This article was submitted to Marine Ecosystem Ecology, a section of the journal Frontiers in Marine Science

Received: *24 September 2019*
Accepted: *27 April 2020*
Published: *25 May 2020*

Citation:
Lichtenberg M, Cartaxana P and Kühl M (2020) Vertical Migration Optimizes Photosynthetic Efficiency of Motile Cyanobacteria in a Coastal Microbial Mat. Front. Mar. Sci. 7:359. doi: 10.3389/fmars.2020.00359

INTRODUCTION

Light-exposed coastal sediments in shallow waters and intertidal areas are often colonized by benthic microalgae and cyanobacteria, which under the absence of animal grazing (typically under environmental extremes such as desiccation, high salinity or sulfide levels) can form complex stratified microbial biofilm communities, i.e., microbial mats (Stal, 1995), that stabilize the sediment by excretion of exopolymers. Microbial mats are densely populated and highly compacted, vertically stratified microbial communities characterized by steep gradients of physical (light and temperature) and chemical parameters (Kühl et al., 1996; Dillon et al., 2009; Al-Najjar et al., 2012; De Beer and Stoodley, 2013). The uppermost layers of coastal microbial mat layers are typically dominated by diatoms on top of a dense green cyanobacterial layer that is often dominated

by *Microcoleus chtonoplastes* and various other motile, filamentous cyanobacteria (Wieland et al., 2003; Fourcans et al., 2004; Dillon et al., 2009). Often, purple sulfur bacteria and green filamentous anoxygenic phototrophs are found below the cyanobacteria followed by a reduced black layer of precipitated iron sulfide (Jørgensen, 1982). Besides light-driven sulfide oxidation by anoxygenic phototrophs, sulfide can also be oxidized efficiently by colorless sulfur bacteria such as filamentous *Beggiatoa* spp. (Nelson and Castenholz, 1981) that are motile and produce white patches in the microbial mat at the oxygen-sulfide interface (Jørgensen and Revsbech, 1983).

Light is the primary energy source for photosynthetic microbial mats. Due to the high density of photopigments, organic matter, and sediment particles, light is subject to intense scattering and absorption within microbial mats (Kühl and Jørgensen, 1994; Kühl et al., 1994). This can lead to an extremely narrow photic zone (Kühl et al., 1997) and a rapid change in spectral composition with depth (Lassen et al., 1992; Cartaxana et al., 2016b). Ploug et al. (1993) related changes in light quality in a coastal microbial mat to the vertical zonation of a population of diatoms over a dense filamentous cyanobacteria layer that largely sustained their oxygenic photosynthesis via phycobiliproteins with absorption characteristics complementary to chlorophylls. Similarly, complementary use of visible and near-infrared radiation by chlorophylls/phycobilins vs. bacteriochlorophylls enables coexistence of dense populations of oxygenic phototrophs on top of anoxygenic phototrophs (Kühl and Fenchel, 2000). Apart from light, other parameters such as nutrient availability or the presence of sulfide may vertically limit photosynthesis in microbial mats (Stal, 1995; Kühl et al., 1996; Wieland et al., 2003).

The ecological success of benthic microbes in optically dense and vertically stratified communities has recurrently been linked to cell motility allowing individual microbes to search for optimal environmental conditions regarding crucial parameters such as light, temperature, O_2 or nutrient availability (Whale and Walsby, 1984; Bebout and Garcia-Pichel, 1995; Bhaya, 2004; Serôdio et al., 2006). Complex migratory rhythms determined by day/night cycles, tidal regimes, UV exposure and changes in irradiance levels have been described for both diatom- and cyanobacteria-dominated phototrophic mat communities (Bebout and Garcia-Pichel, 1995; Serôdio et al., 2006; Coelho et al., 2011). Similar strategies to optimize photon capture are known in terrestrial plants, where the position of chloroplast in palisade and mesophyll layers in leaves can change depending on light levels and light field directionality, i.e., diffuse versus collimated light (Vogelmann, 1993; Gorton et al., 1999; Wada et al., 2003). Raphidic diatoms, filamentous cyanobacteria and *Beggiatoa* spp. are able to glide within an extracellular polymeric matrix at speeds of 0–10 $\mu m\ s^{-1}$ (Glagoleva et al., 1980; Richardson and Castenholz, 1987; Hoiczyk, 2000; Gupta and Agrawal, 2007; Kamp et al., 2008; Tamulonis et al., 2011). Because of the steep light gradient, migration and the resultant vertical redistribution of the productive biomass have important consequences for both the photobiology of the phototrophs and the net primary productivity of the microbial mat ecosystem (Bebout and Garcia-Pichel, 1995; Cartaxana et al., 2016b).

Recent studies have focused on the efficiency with which light is utilized and converted to chemical energy via photosynthesis in cyanobacterial mats and mixed cyanobacteria-diatom biofilms (Al-Najjar et al., 2010, 2012). In these studies, relatively low photosynthetic efficiencies were estimated for microbial mats compared with ecosystems with a more open canopy-like organization such as coarse sediments (Lichtenberg et al., 2017), macroalgal stands (Sand-Jensen et al., 2007), corals (Brodersen et al., 2014), or terrestrial forest communities (Terashima et al., 2016), where light propagation is not hindered to the same extent by self-shading and photosynthetic inactive components. How the photosynthetic efficiency of biofilms and microbial mats is modulated by the migration of motile phototrophic populations remains to be studied in detail. In this study, we used fiber-optic scalar irradiance and field radiance microprobes in combination with O_2 and temperature microsensors to investigate the radiative energy budget for the euphotic zone in a coastal microbial mat dominated by motile cyanobacteria and colorless sulfur bacteria. We investigated how photosynthetic efficiency of oxygenic phototrophs in the microbial mat was affected by changes in vertical biomass distribution imposed by acclimating the microbial mat to different light conditions.

MATERIALS AND METHODS

Sample Collection and Preparation

Microbial mats were collected from a periodically desiccated sand flat in Aggersund, Limfjorden, Denmark. The water level at the sample site is mainly determined by wind and local current patterns, and the mats can experience desiccation for extended periods. The sampled mats were dark green/black in appearance and were dominated by filamentous cyanobacteria (*Microcoleus* spp. and other motile morphotypes). Beneath the cyanobacterial band, a population of the sulfur bacteria *Beggiatoa* spp. was found. See Nielsen et al. (2015) for more details of the microbial mat and sampling site.

Mat samples were collected using small plastic trays ($7 \times 2 \times 5$ cm) and were brought back to a field laboratory (Rønbjerg Marine Research Station, Aarhus University, Denmark), where they were incubated submerged in seawater (20°C; Salinity = 27) under a low photon irradiance (∼75 μmol photons $m^{-2}\ s^{-1}$) of photosynthetically active radiation (PAR, 400–700 nm) provided by a halogen lamp. Within few hours of incubation, the mat turned dark green as motile cyanobacteria aggregated and extensive bubble formation from oxygenic photosynthesis appeared on the surface of the mat.

During measurements, the mat samples were transferred to a flow chamber ($25 \times 8 \times 8$ cm) that provided a stable laminar flow (∼2 cm s^{-1}) of aerated seawater (room temperature = 21–23°C; Salinity = 27) (see also Brodersen et al., 2014; Lichtenberg et al., 2017) that minimized bubble formation due to enhanced mass transfer between the microbial mat and water. The flow chamber was connected to a 25 L aquarium where water was recirculated through. Light was provided vertically from above by a white LED lamp (KL-2500 LED, Schott, Germany; color temperature of 5600K) equipped with a collimating lens. The incident irradiance

(400–700 nm) from the lamp was regulated electronically without spectral distortion. The downwelling photon irradiance was measured with a calibrated photon irradiance meter (ULM-500, Walz GmbH, Germany) equipped with a factory-calibrated photon irradiance detector (LI-192S, LiCor, United States). Incident spectral irradiance was also measured in radiometric units (W m^{-2} nm^{-1}) with a calibrated spectroradiometer (Jaz ULM, Ocean Optics, United States). All sensors were mounted in a 45° angle (relative to the vertically incident light) on a motorized micromanipulator (MU-1, PyroScience, Germany), which could be controlled by the manufacturer's software (Profix, PyroScience, Germany). All measurements were performed under an incident photon irradiance (400–700 nm) of 1000 μmol photons m^{-2} s^{-1} as provided by the white LED lamp. This light level was chosen as a saturating irradiance based on a previously measured photosynthesis – irradiance curve (PI). For each profile a new horizontal position in a mat was randomly chosen. Prior to measurements, the vertical distribution of biomass was modulated by incubating the biofilm samples for at least 3 h in either darkness, low light (∼75 μmol photons m^{-2} s^{-1}) or high light (1000 μmol photons m^{-2} s^{-1}), respectively. Upon increasing the irradiance to 1000 μmol photons m^{-2} s^{-1}, scalar irradiance and gross photosynthesis were measured immediately, reflecting the systems immediate response to the new irradiance. Profiles of O_2 and temperature were illuminated for 10 min at 1000 μmol photons m^{-2} s^{-1} before measurements, and we note that the mats were therefore not measured under steady state (see also discussion).

Light Measurements

Spectral scalar irradiance was measured with a fiber-optic scalar irradiance microprobe (spherical tip diameter ∼70 μm) (Rickelt et al., 2016) connected to a fiber-optic spectrometer (USB2000+, Ocean Optics, United States). Spectral downwelling irradiance, $E_d(\lambda)$, was measured with the microprobe tip positioned in a black, non-reflective, light-well at the same distance from the light source as the mat surface (see **Table 1** for definition of abbreviations). In the mat samples, spectral scalar irradiance, $E_0(\lambda)$ was measured in vertical increments of 0.1 mm. These measurements were then corrected for exposure time of the spectrophotometer and normalized to similarly corrected downwelling irradiance spectra yielding scalar irradiance transmittance spectra in different mat layers in % of $E_d(\lambda)$, i.e., $100 \cdot E_0(\lambda)/E_d(\lambda)$.

Spectral attenuation coefficients of scalar irradiance, $K_0(\lambda)$ were calculated for specific depth intervals in the microbial mats as (Kühl, 2005):

$$K_0(\lambda) = -ln\frac{(E_0(\lambda)_1/E_0(\lambda)_2)}{z_2 - z_1}$$

where $E_0(\lambda)_1$ and $E_0(\lambda)_2$ are the spectral scalar irradiances measured at depth z_1 and z_2, respectively.

Similarly, depth profiles and attenuation coefficients of PAR, K_0, were calculated from integrated values over the spectral region of interest. Light measurements <420 nm exhibited noisy signals and increasing amounts of stray light from within the detector and integrations were therefore carried out from 420–700 nm (henceforth mentioned as PAR). In deeper layers of the mat, integration of the measurements encompassed regions in the blue part of the spectrum exhibiting very noisy signals and an increasing contribution from stray light in the spectrometer, and these noisy signals were therefore excluded.

Reflectance of the microbial mat surface was measured with a fiber-optic field radiance miniprobe (flat cut tip diameter = 1 mm) connected to the same fiber-optic spectrometer used for scalar irradiance measurements. The PAR reflectance (R_{PAR}) was calculated from the upwelling irradiance [$E_u(\lambda)$], here measured as the backscattered spectral radiance assuming Lambertian (diffuse) backscatter from the mat surface (Kühl and Jørgensen, 1994), and the downwelling irradiance [$E_d(\lambda)$] measured as the backscattered spectral radiance measured over a white Lambertian reflectance standard (99%; Spectralon, Labsphere, United States) as (Kühl, 2005):

$$R_{PAR} = \int_{420}^{700} \frac{E_u(\lambda)}{E_d(\lambda)} d\lambda$$

The acceptance angle of light collection through the fiber depends on the numerical aperture (NA) of the fiber and the refractive index of the medium. Since $E_d(\lambda)$ was estimated in air, and $E_u(\lambda)$ was measured in water we corrected for the acceptance angle differences by the relation $\Theta_a = sin^{-1}\left(\frac{NA}{RI_w}\right)$, where Θ_a is the acceptance angle, NA is the numerical aperture of the fiber (0.22) and RI_w is the refractive index of water (1.33).

Microsensor Measurements of O_2 Concentration and Gross Photosynthesis

Vertical depth profiles of O_2 concentration were measured using Clark-type O_2 microelectrodes (tip diameter = 25 μm, OX-25, Unisense A/S, Aarhus, Denmark) with fast response time (<0.5 s) and low stirring sensitivity (<1–2%) (Revsbech, 1989), connected to a pA-meter (Unisense A/S, Aarhus, Denmark) and interfaced through an A/D converter (DCR-16, PyroScience, Germany) to data acquisition software (Profix, PyroScience, Germany). The O_2 signals were also recorded on a strip-chart recorder (BD 12E; Kipp & Zonen BV, Netherlands) connected to the pA-meter. Sensor signals were linearly calibrated at experimental temperature and salinity from measurements in the aerated free flowing water in the flow-chamber and in anoxic zones in the sediment. Depth profiles of O_2 concentration were measured in 0.1 mm increments relative to the mat surface position determined by placing the sensor tip at the mat surface (z = 0 mm), as observed through a USB microscope (AM7013MZT Dino-Lite, AnMo Electronics Corporation, Taiwan). The sensor tip was then moved to 1.5 mm above the mat surface ($z = -1.5$ mm) and from here profiles were measured in steps of 100 μm until reaching anoxic mat layers (z∼1.5 mm).

The volume-specific rate of gross photosynthesis [PS(z) in nmol O_2 cm^{-3} s^{-1}] was measured using the light/dark shift method (Revsbech and Jørgensen, 1983) in vertical steps of 0.1 mm starting from just above the microbial mat surface until the depth where no immediate O_2 signal changes were observed upon darkening. Areal rates of gross photosynthesis [PS(a) in

nmol O_2 cm^{-2} s^{-1}] were calculated by integrating the volumetric rates over depth.

Temperature Microsensor Measurements

Temperature profiles were measured using thermocouple microsensors (tip diameter = 50 μm, TP-50, Unisense A/S, Aarhus, Denmark) connected to a thermocouple meter (Unisense A/S, Aarhus, Denmark) and interfaced through an A/D converter (DCR-16, PyroScience, Germany) to data acquisition software (Profix, PyroScience, Germany). Signals were linearly calibrated against a high precision digital thermometer (± 0.2°C; Testo 110, Testo AG, Germany) in seawater of different temperatures. The areal heat dissipation from the microbial mat was calculated using Fourier's law of conduction using the linear temperature gradient in the thermal boundary layer (TBL) and the thermal conductivity of seawater (k = 0.6 W m^{-1} K^{-1}):

$$J_H = k\frac{\partial T}{\partial z}$$

The downward heat dissipation could not be directly calculated from the measured temperature profiles, and were estimated from the principle of energy conservation as the difference between the absorbed light energy and the sum of photosynthesis and upward heat flux (both in energy units).

Energy Calculations

To obtain absolute scalar irradiance spectra, we multiplied the measured transmittance spectra for each depth with the measured incident radiometric spectra (in W m^{-2}). By using Planck's equation:

$$E_\lambda = h\,\frac{c}{\lambda},$$

where E_λ is the energy of a photon with a wavelength λ, h is Planck's constant ($6.626 \cdot 10^{-34}$ W s^2) and c is the speed of light in vacuum (in m s^{-1}), we then converted absolute scalar irradiance spectra to absolute spectra of photon scalar irradiance [$E_0(z)$ in μmol photons m^{-2} s^{-1} nm^{-1}].

The total absorbed light energy in the mat (J_{ABS} in J m^{-2} s^{-1}), i.e., the vector irradiance, was calculated from the downwelling spectral irradiance $E_d(\lambda)$ and the irradiance reflectance as:

$$J_{ABS} = \int_{420}^{700} E_d(\lambda)(1 - R(\lambda))d\lambda$$

The amount of energy dissipated via photosynthesis was calculated by multiplying the areal photosynthesis rates [PS(a)] with the Gibbs free energy from the light reactions, where O_2 is produced by the photolysis of water. Including the formation of ATP this yields 482.9 kJ (mol O_2) $^{-1}$ (Thauer et al., 1977).

Energy budgets for the entire photic zone were calculated under the assumption that the total energy stored in photosynthesis (J_{PS}), and dissipated via heat (J_H) and reflection (R) balanced the incoming radiative energy (J_{IN}):

$$J_{IN} = J_H + J_{PS} + R \text{ and } J_{IN} - R = J_{ABS} = J_H + J_{PS}$$

To investigate how photosynthetic quantum efficiency varied with depth in the microbial mat, we calculated relative photosynthetic efficiencies (in mol O_2 (mol photons) $^{-1}$ mm^{-1}) by dividing the photosynthetic rates in a specific depth layer with the photon scalar irradiance just above that layer (Lassen et al., 1992). We note that the calculated efficiency parameter does not reflect the true quantum efficiency, where depth specific photosynthesis is related to the number of absorbed photons in that particular depth (see section Discussion).

HPLC Pigment Analysis

Sediment samples of the 0-0.5 mm surface layer were collected using the "crème brûlée" sampler described by Laviale et al. (2015) and stored at −80°C. Approximately 100 mg of sampled mat material were ground with a micro pestle and extracted in a mixture of acetone and methanol (7:2). Samples were sonicated (S-4000, Branson Ultrasonic Corporation, United States) for 20 s to improve pigment extraction and were then centrifuged for 60 s at 13,400 rpm. Supernatants were filtered through 0.45 μm PTFE-membranes and immediately injected in a HPLC (1260 Infinity, Agilent Technologies, United States). Fifteen microliter of 1 M ammonium acetate was added to each HPLC vial prior to injection as a resolution-improving agent. The solvent gradient was set up according to Frigaard et al. (1997) with a 69 min elution program, a flow rate of 1.0 mL min^{-1} and an injection volume of 100 μL. Chromatographic separation was carried out using a C18 Ascentis column for reverse phase chromatography (5 μm particle size; L × I.D: 25 cm × 4.6 mm). Pigments were identified from their characteristic retention times and absorbance spectra.

RESULTS

Light, Temperature, and Photosynthesis

Microprofiles of photon scalar irradiance in the dense microbial mat were measured after incubation in dark, low light (75 μmol photons m^{-2} s^{-1}), and high light (1000 μmol photons m^{-2} s^{-1}), respectively, which yielded a different spatial organization of motile microbes in the mat (**Figure 1**). In the low light-acclimated state, a cyanobacterial layer formed near the surface, while in the high light-acclimated state the cyanobacteria were found in deeper layers. In the dark-acclimated mat, a dense whitish layer of colorless *Beggiatoa* spp. formed at the surface with the cyanobacteria located just below the colorless sulfur bacteria (**Figure 1**).

The vertical attenuation of photosynthetically active radiation (PAR, 400–700 nm) with depth in the microbial mat did not follow a mono-exponential decay, but exhibited variable attenuation in different layers depending on light acclimation and the distribution of biomass in the mat (**Figures 2A–C**). In the low light acclimated state, the strongest attenuation of PAR was found in the top 0.2 mm (K_0 = 13.9 mm^{-1}), whereas the underlying part of the microbial mat (0.3–0.5 mm) showed a slightly lower attenuation of PAR scalar irradiance (K_0 = 10.3 mm^{-1}). In the high light-acclimated state this trend was reversed, where the attenuation of PAR in the top layer (K_0 = 10.6 mm^{-1}) was lower

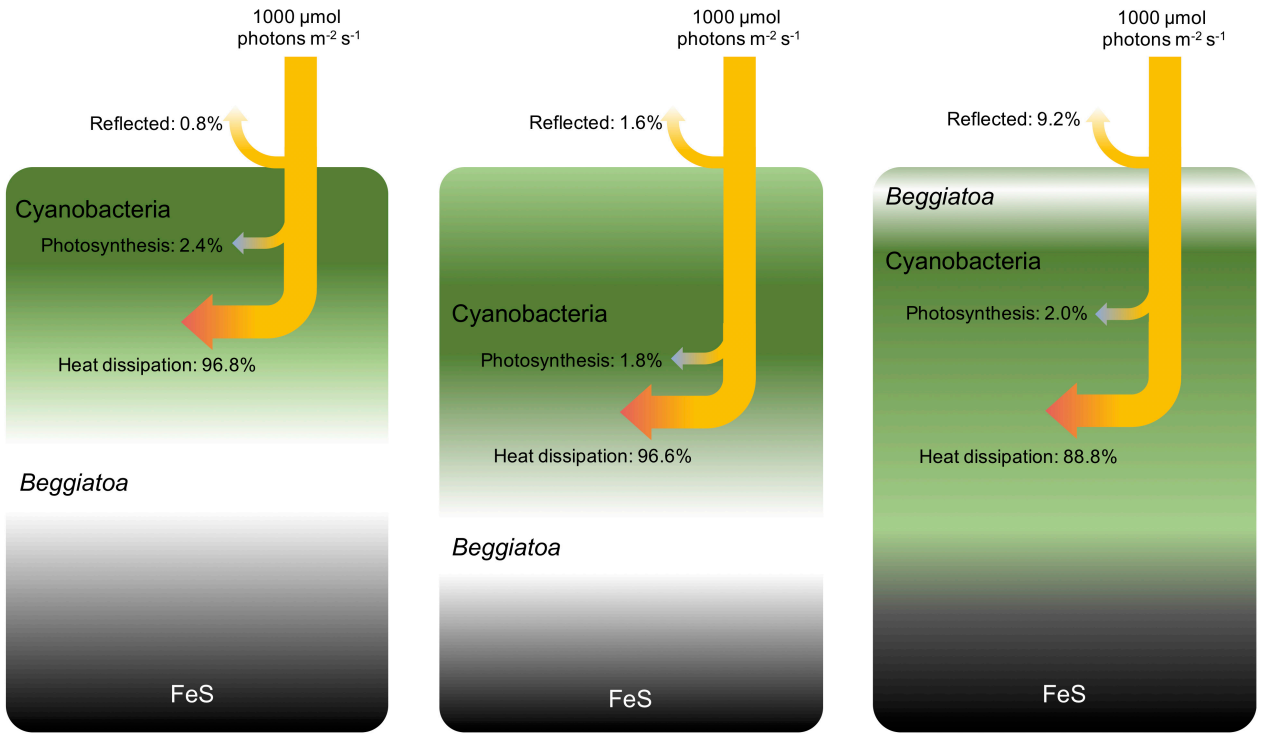

FIGURE 1 | Conceptual drawing of the biomass distribution during different light acclimation scenarios and the corresponding radiative energy budgets of the entire photic zone measured under an incident photon irradiance of 1000 µmol photons m^{-2} s^{-1}. The surface layers of the microbial mat were dominated by dense populations of motile cyanobacteria (*Microcoleus* sp. and other filamentous species) and filamentous sulfide oxidizing bacteria (*Beggiatoa* spp.). Beneath the narrow photic zone, a dark FeS-containing sediment layer was present. In low light, the upper layers became oxidized driving the O_2-H_2S interface and thus *Beggiatoa* deeper into the mat, while the motile cyanobacteria moved toward the mat surface under non-inhibitory light levels. In high light, a larger part of the biofilm is oxidized, *Beggiatoa* moved further down, while motile cyanobacteria in the top layers started to move downwards to avoid high photoinhibitory light levels at the microbial mat surface. In darkness, the entire mat became anoxic and the *Beggiatoa* moved to the mat surface forming a white layer on top of the cyanobacteria, to avoid the high levels of H_2S and remain at the O_2-H_2S interface (Preisler et al., 2007), whereas the cyanobacteria remained in a dense layer underneath.

than in deeper layers of the microbial mat (K_0 = 16.5 mm^{-1}). In the dark-acclimated state, a lower attenuation of PAR was found in the top 0.2 mm (K_0 = 5.8 mm^{-1}) of the microbial mat followed by a very steep attenuation from 0.2 to 0.4 mm depth (K_0 = 22.2 mm^{-1}).

Spectral attenuation of scalar irradiance in the PAR region was enhanced around absorption maxima of most abundant photopigments commonly found in cyanobacterial mats, e.g., Chl *a* (440 nm; 675 nm), phycocyanin (620 nm) and phycoerythrin (565 nm) (**Figures 2D–F**). HPLC analysis revealed the presence of other cyanobacterial pigments such as myxoxanthophyll, zeaxanthin, oscillaxanthin and β,ε-carotene in the upper 0.5 mm of the mat, along with BChl *a* indicative of anoxygenic phototrophs (**Figure 3**). Due to the strong light attenuation in the mat, <1% of PAR surface scalar irradiance remained just 0.4 mm below the biofilm surface (**Figure 2**). The very high light-attenuation of PAR (400–700 nm) and dense pigmentation of the microbial mat resulted in low surface reflection (**Figure 1**). In the low-light acclimated state, only 0.75% of the incident light was reflected, whereas the reflection from the mat surface in the high light-acclimated state was twice as high (1.6%). In the dark-acclimated state, where the surface of the microbial mat was covered by a whitish layer of motile, filamentous colorless sulfur bacteria (*Beggiatoa* spp.), the reflection increased ∼10-fold to 9.2% of the incident irradiance.

Most of the incident irradiance in the PAR region was thus readily absorbed in the mat, and the majority of the absorbed light was dissipated as heat as quantified from the heat flux over a ∼1.2 mm thick thermal boundary layer (TBL) (**Figure 4**). Under similar flow and thus TBL thickness, the mat surface heating differed slightly depending on light acclimation, where the surface temperature of the high light-acclimated mat increased by 0.3°C as compared to the low light-acclimated mat showing a mat surface temperature increase of 0.24°C. Lowest surface heating was measured when illuminating the dark-acclimated mat reaching a surface temperature increase of 0.2°C.

Due to the high light-attenuation, the euphotic zone of the microbial mat was restricted to the uppermost 0.6 to 0.8 mm (**Figure 5**). The depth distribution of gross photosynthesis rates varied with light acclimation, and very high rates were observed

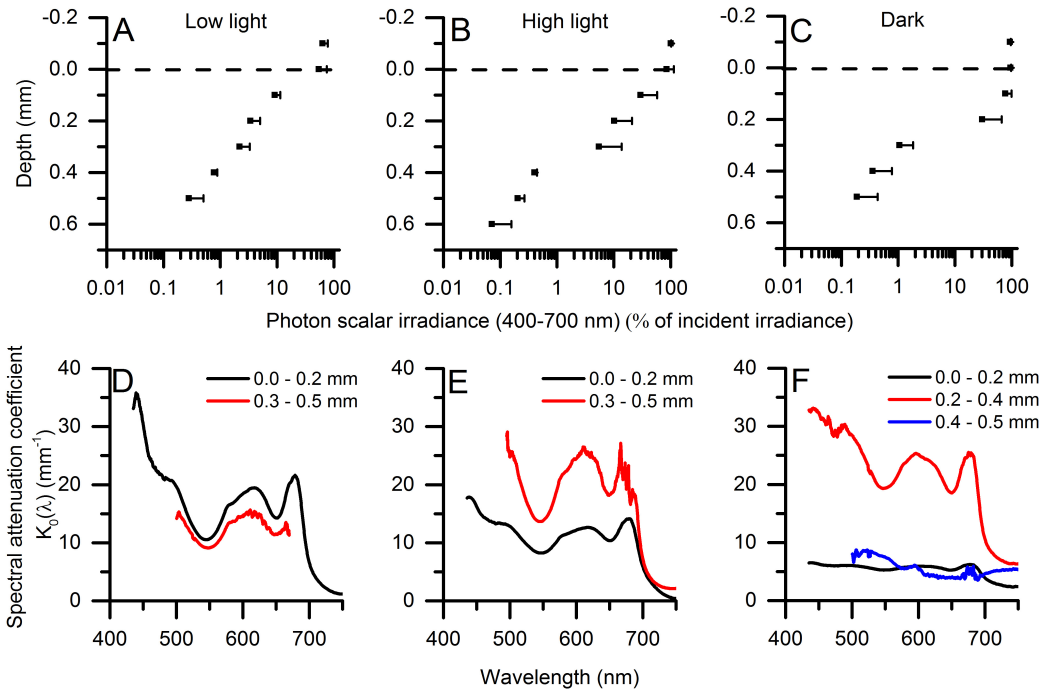

FIGURE 2 | (A–C) Vertical microprofiles of photon scalar irradiance (PAR; 420–700 nm) (in μmol photons m^{-2} s^{-1}). The dashed line indicates the biofilm surface. [means ± 1 SD (only + SD shown for clarity); n = 3]. PAR attenuation coefficients, K_0, were estimated in the upper- and lower part of the biofilm (0.0–0.2 mm; 0.3–0.5 mm) from the slope of linear regressions on natural logarithm transformed data (R^2 > 0.95 for all plots). **(D–F)** Shows spectral attenuation coefficients, $K_0(\lambda)$ (in mm^{-1}) in different zones of the biofilm (n = 3). The measurements were done in low light-acclimated (left panels), high light-acclimated (middle panels), and dark-acclimated biofilms (right panels). At depth in the mats, very low light levels led to decreasing signal to noise ratios and increasing contributions by straylight in the spectrometer at shorter wavelengths and spectra were therefore truncated.

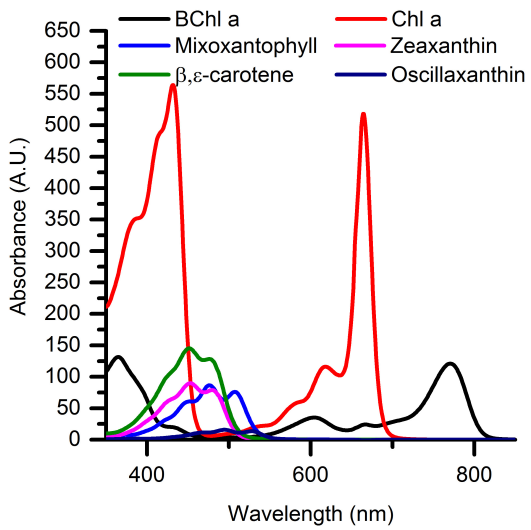

FIGURE 3 | Relative absorbance spectra of predominant photopigments found in the upper 0.5 mm of the microbial mat as investigated with HPLC analysis.

in all treatments (up to 30 nmol O_2 cm^{-3} s^{-1}). In the low light-acclimated state, peaks of gross photosynthesis were found at the mat surface and 0.3 mm beneath the surface. In the high light-acclimated state, the photosynthetic rates near the surface were diminished, while a stronger sub-surface peak in gross photosynthesis was found around 0.2 mm below the mat surface. The dark-acclimated mat showed a small photosynthesis peak near the mat surface and a sub-surface peak at 0.3–0.4 mm depth (**Figure 5**). However, the O_2 concentration profiles between light acclimations were quite similar and did not show any clear differences in e.g., O_2 penetration depth (**Figure 5**).

Energy Budgets

The vector irradiance, i.e., the net downwelling radiative energy flux (400–700 nm), was very similar between light acclimations and amounted to 218.0 ± 5.6 W m^{-2}. However, the heat dissipation from the mat to the water differed between light incubations, where the dark-acclimated mat exhibited the lowest upward heat dissipation of 140 W m^{-2}, the heat dissipation in the low light-acclimated mat was 144 W m^{-2}, and the highest heat dissipation was measured in the high light-acclimated mat reaching 179 W m^{-2}.

Depth integrated gross (oxygenic) photosynthesis only accounted for a small part of the absorbed light energy. The highest amount of radiative energy stored via photosynthesis was measured in the low light-acclimated microbial mat and amounted to 5.4 ± 0.7 W m^{-2}, while the high light- and the dark-acclimated mat conserved 4.06 ± 1.6 W m^{-2} and 4.8 ± 1.1 W m^{-2}, respectively.

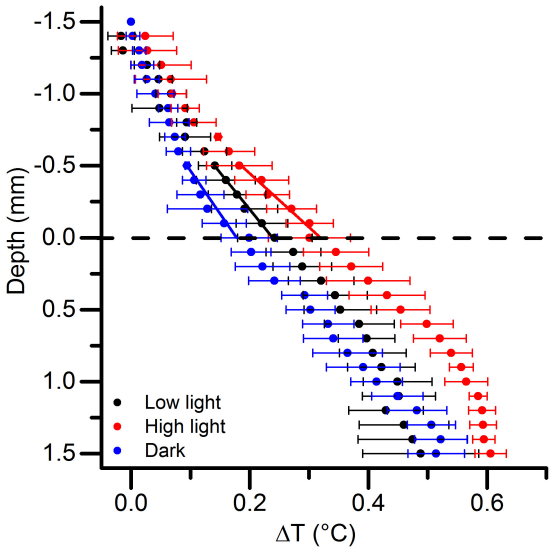

FIGURE 4 | Vertical microprofiles of temperature increase (ΔT in°C) relative to the free-flowing water temperature under an incident photon irradiance of 1000 μmol photons m^{-2} s^{-1}. The dashed line indicates the microbial mat surface. Black, red, and blue symbols represent measurements in a low light-, high light-, and dark-adapted mats, respectively. The straight black, red and blue lines indicate the linear regressions used to estimate the areal heat dissipation from the microbial mat. Data points with error bars represent means ± 1 SD (n = 3).

Relative to the incident energy, the photosynthetic energy conservation efficiency for the entire photic zone thus only accounted for ∼2% (2.1, 2.4, and 1.8% for the dark-, low light-, and high light-acclimated biofilm, respectively), while the majority of incident light energy was dissipated as heat (**Figure 1**).

Relative Photosynthetic Efficiencies

Depth profiles of relative photosynthetic efficiencies in the microbial mat were calculated by normalizing the measured volumetric gross photosynthesis rates at each depth to the scalar irradiance incident to that depth. Such profiles showed sub-surface peaks in relative photosynthetic efficiency in all light acclimation states of the microbial mat (**Figure 6**). In the low light-acclimated mat, a peak in relative efficiency was located closest to the surface at 0.3 mm depth. The dark-acclimated mat exhibited highest relative photosynthetic efficiencies 0.4 mm beneath the surface, while the highest relative photosynthetic efficiencies in the high light acclimated mat were found near the lower boundary of the photic zone at 0.5 mm below the mat surface.

DISCUSSION

Radiative energy budgets in microbenthic systems have previously been studied in cyanobacterial mats and biofilms (Al-Najjar et al., 2010, 2012), sediments (Lichtenberg et al., 2017), and corals (Brodersen et al., 2014), albeit under the assumption of a homogenous depth distribution of biomass. In the studied microbial mat, dense populations of phototrophic microalgae and cyanobacteria reside in steep gradients of resource stratification shaped by communities of photo-, chemo-, and heterotrophic microorganisms creating a steep redox gradient (van Gemerden, 1993). Consequently, the physical and chemical landscape in such microbial mats can change, within less than one mm, from intense sun exposure (>1000 μmol photons m^{-2} s^{-1}) and O_2 supersaturation (up to 2 mM) to complete darkness and a reduced anoxic sediment high in H_2S (Jørgensen, 1982).

The studied microbial mat exhibited an extremely high optical density and attenuation of PAR, where >99% of the surface irradiance was effectively absorbed <0.4 mm below the microbial mat surface. Light was thus the primary limiting resource for microbial phototrophs in the mat. One strategy to remain competitive under light limitation is to complement light absorption by Chl *a*, the main light harvesting pigment in oxygenic photosynthesis, by metabolic investment in producing a range of accessory pigments absorbing a broader part of the available light spectrum and channeling it to the photosynthetic reaction centers (Stomp et al., 2007; Trampe and Kühl, 2016; Kühl et al., 2020). HPLC pigment analysis of the upper 0.5 mm of the microbial mat revealed that very efficient light absorption was achieved by a mixture of light harvesting pigments from cyanobacteria (Chl *a*, mixoxanthophyll, zeaxanthin, oscillaxanthin and β,ε-carotene) and anoxygenic phototrophs (BChl *a*), able to absorb light from the UV-B well into the NIR region (**Figure 3**). We did not find any signs of typical diatom light harvesting pigments (fucoxanthin, diadinoxanthin or Chl *c*) or the far-red absorbing chlorophylls *d* or *f* in either measurements of scalar irradiance or by HPLC analysis.

The attenuation of light was stratified with depth and varied between the different acclimation states. In all acclimations, we found strong spectral attenuation from typical cyanobacterial pigments confirmed by the HPLC pigment analysis. In low light acclimated mats the strongest spectral attenuation was in the top 0.2 mm while the strongest spectral attenuation was found deeper (0.3–0.5 mm) in the high light acclimated mats.

Consequently, low surface reflection was observed in the low and high light-acclimated microbial mats. In the low light-acclimated mat, the cyanobacterial population was located near the surface and only 0.75% of the incident irradiance was backscattered, while in the high light-acclimated state, the motile cyanobacteria migrated downward changing the surface biomass composition leading to higher reflectance. During dark-acclimation, the surface of the biofilm became anoxic and a layer of the motile, filamentous colorless sulfur bacteria *Beggiatoa* formed on the mat surface. *Beggiatoa* spp. are sulfide oxidizing bacteria known to store granules of elemental sulfur (Nelson and Castenholz, 1981), which make the filaments appear white due to strong light scattering, which in our measurements increased the surface reflectance to 9.2% of the incident irradiance. Multiple scattering in sediments and coral tissues have previously been shown to increase the scalar irradiance in top layers (Kühl and Jørgensen, 1994; Wangpraseurt et al., 2012) which could explain the very low attenuation of light in the top layers of the dark-acclimated mat (**Figure 2**). Light-dependent migration

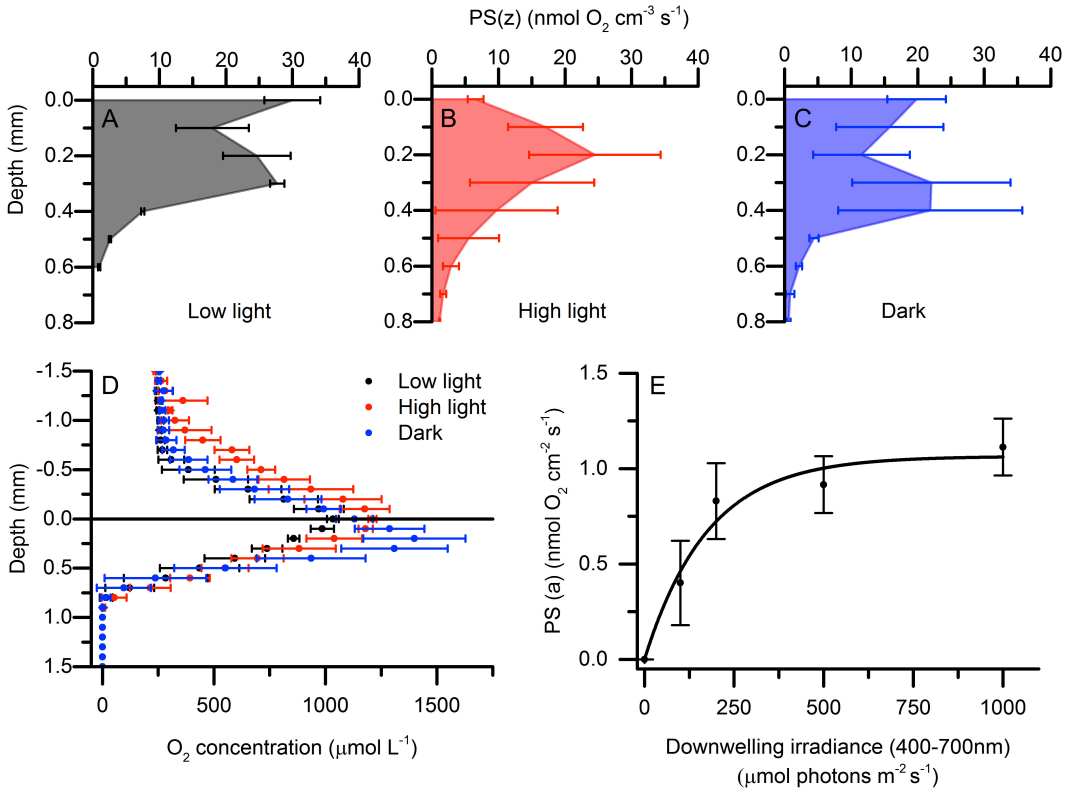

FIGURE 5 | Depth distribution of volumetric gross photosynthesis rates [PS(z)] under an incident photon irradiance of 1000 µmol photons m^{-2} s^{-1}. Measurements were done in a low light-acclimated **(A)**, high light-acclimated **(B)**, and dark-acclimated **(C)** microbial mat. Data points with error bars represent means ± 1 SD (n = 3). **(D)** Depth profiles of O_2 concentration in low light, high light, and dark acclimated microbial mats measured under a downwelling photon irradiance (400–700 nm) of 1000 µmol photons m^{-2} s^{-1}(means ± 1SD; n = 3). **(E)** Areal photosynthetic rates [PS(a)] vs. irradiance curve using 30 min acclimation to each irradiance (means ± 1 SD; n = 3). Data was fitted with an exponential saturation model (Webb et al., 1974).

patterns of cyanobacteria and *Beggiatoa* thus clearly modulated the radiative energy input to the microbial mat.

The strong light absorption in the uppermost mat layers, resulted in very high local photosynthetic rates reaching >30 nmol O_2 cm^{-3} s^{-1}. This is about 2–5 fold higher than rates measured in most other cyanobacteria-dominated microbial mats (Al-Najjar et al., 2012), but e.g., comparable to rates measured in a highly stratified intertidal mudflat community dominated by motile diatoms (Cartaxana et al., 2016b) and in a cultivated diatom biofilm (Jensen and Revsbech, 1989). We investigated photosynthesis under high light exposure of microbial mats exhibiting different distributions of motile microbes in response to different light history. Investigations of photosynthesis under increasing irradiances in motile microbial systems are complex as migrating cells under changing light can change the spatial characteristics of the biofilm/mat and thereby potentially affect light exposure and distribution in different mat layers (Kühl et al., 1997). In the present study, the main aim was thus to investigate how the migration of motile cyanobacteria affected photosynthetic efficiency under different spatial organization of phototrophs in the microbial mat.

This is experimentally challenging, and we note that these measurements were not performed under steady-state conditions. The change to higher light than the acclimation irradiance will start to move the mat toward a new steady-state and rates and profiles will thus be measured under transient "quasi steady-state" conditions. The measurements of scalar irradiance and gross photosynthesis reflect the community's response to high light in the current distribution of biomass. The distribution of O_2 and temperature is, however, more complex to interpret, as the distribution of O_2 is determined by the interplay between diffusion, production and consumption, while the temperature profiles are determined by the local heat dissipation and heat transfer properties. These are slower processes and will move toward a steady state on the same time scale as motility driven biomass redistribution in such compact systems as the studied mats.

Areal rates of oxygenic photosynthesis, integrated across the entire euphotic zone, did not differ markedly between different light acclimations (0.99, 1.11, and 0.84 nmol O_2 cm^{-2} s^{-1} for dark-, low light- and high light-acclimated samples, respectively) under the high saturating photon irradiance used for the energy budget measurements. It is however noted that the lowest areal photosynthetic rates were observed in the high light-acclimated state. One could speculate that the longer acclimation period to high light could have given the phototrophs, in this treatment,

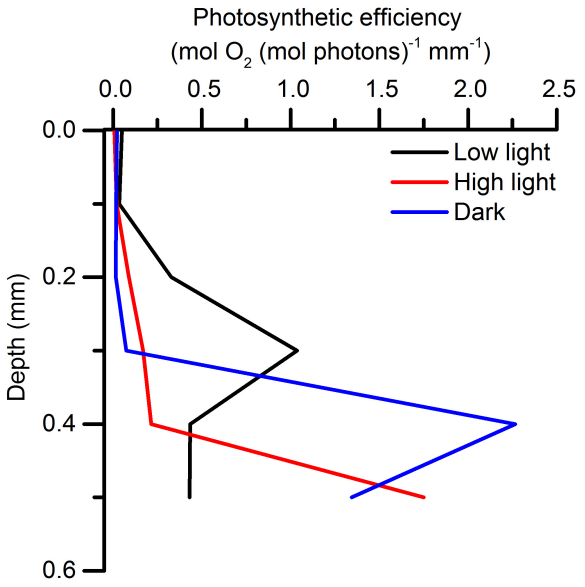

FIGURE 6 | Photosynthetic efficiencies [in mol O_2 (mol photons) $^{-1}$ mm^{-1}] calculated from volume-specific gross photosynthesis rates and the photon scalar irradiance incident to the corresponding depth in a low light-, high light-, and dark-acclimated biofilm (means; $n = 3$).

time to adjust their balance between photosynthesis and non-photochemical quenching (NPQ) processes. One of the most important short-term regulatory mechanisms to avoid photo damage is NPQ, where excess energy decays from singlet excited chlorophyll (^{1}Chl*) into heat dissipation (Müller et al., 2001). This mechanism significantly lowers the effective quantum yield of photosynthesis but avoids the formation of reactive singlet oxygen ($^1O_2$*) by the triplet state of chlorophyll (^{3}Chl*) (Müller et al., 2001), which can have long term detrimental effects on the photosystems by degradation of the D1 protein; an important component in photosystem II (Nymark et al., 2009). The higher rates displayed by the top population for the dark- and low-light acclimated mats could therefore be a product of the more open reaction centers before regulating the different NPQ components that operate on time scales from a few minutes to a few hours (Kress and Jahns, 2017).

Photophobic responses or phototaxis enabling movement along a light gradient (Jekely, 2009) are alternative strategies of photoprotection, enabling motile phototrophs to align their position at optimum irradiance in light gradients (Tamulonis et al., 2011) depending on the status of the electron transport chain and time of the day (Burns and Rosa, 1980). *Microcoleus chtonoplastes* displays light dependent migration preferring moderate to low light levels (Ramsing and Prufert-Bebout, 1994), and other studies have found that as little as a 4% difference in light intensity between "head" and "tail" of a cyanobacterial filament can trigger their movement (Häder, 1987). From our measured depth profiles of gross oxygenic photosynthesis, it appears that the distance of vertical migration was limited to only 0.2 to 0.3 mm. However, due to the steep light gradients in the investigated microbial mat, the changes in the light field over such short distances are dramatic, and cyanobacteria migrating 200 μm deeper into the mat experienced a >84-fold decrease in scalar irradiance (**Figure 2C**; 0.4–0.2 mm) from >350 μmol photons m^{-2} s^{-1} to < 10 μmol photons m^{-2} s^{-1}. Such strong changes in light exposure upon migration distances of a few 100 μm have previously been demonstrated in hypersaline cyanobacterial mats (Kühl et al., 1997). Consequently, the spatial distribution of gross photosynthesis varied with light acclimation, probably as a result of migrations of the cyanobacteria and *Beggiatoa*.

Other triggers for migration could also play a role in the observed redistribution of biomass. Sulfide is well known to cause migration due to its cytotoxicity (Whale and Walsby, 1984). Sulfide was most likely present in high concentrations in the studied mats due to i) the black FeS layer below the photic zone, ii) the presence of BChl *a*, indicative of anoxygenic phototrophs that oxidize hydrogen sulfide to sulfur, and the presence of a dense population of *Beggiatoa* known to thrive at the interface of strong O_2 and sulfide concentration gradients. Earlier microsensor measurements in microbial mats from the same sampling site also demonstrated significant sulfide production and light-driven dynamics of O_2, pH and sulfide in the uppermost mat layers (Nielsen et al., 2015). As stated above, *Microcoleus* prefer moderate to low light levels and their migratory behavior is thus probably due to a combination of photophobic movement and sulfide avoidance, although they can grow in H_2S concentrations up to 974 μM (de Wit and van Gemerden, 1987).

Compared to earlier studies of heat dissipation in corals and microbial mats (Jimenez et al., 2008; Al-Najjar et al., 2010; Brodersen et al., 2014), we found a relatively small heat dissipation from the biofilm surface into the water column and the surface temperature of the microbial mat increased by only ~0.3°C. However, the heat dissipation in deeper mat layers was larger than expected. The zone of maximum temperature increase was expected to be found in the same zone as the largest energy deposition, i.e., in the upper few hundred micrometers of the microbial mat, where >90% of the incident light was attenuated. However, the heat dissipation below 0.5 mm depth was in the same order of magnitude as the upward heat dissipation and reached higher temperatures (**Figure 4**). We note that below the dense photic zone, a black layer of precipitated iron sulfide was found, and absorption of light energy in this sediment layer apparently contributed significantly to the heating of the microbial mat, but this remains speculative. While we did not measure temperature deep enough in the sediment to be able to calculate the downward transport of heat, we estimated from the principle of energy conservation that the downward heat flux contributed about 20–50% of the total heat dissipation.

The amount of photochemically conserved energy did not change markedly between different light acclimation states of the microbial mat when investigated at similar high irradiance, despite the higher reflection and lower heat dissipation observed in the dark-acclimated biofilms. Consequently, the photosynthetic energy conservation was 2.1, 2.4, and 1.8% of the incident energy, for dark-, low light-, and high light-acclimated

TABLE 1 | Definition of abbreviations.

Abbreviation	Definition	Unit
TBL	Thermal boundary layer	
PAR	Photosynthetic active radiation (420–700 nm)	
PS(z)	Volume-specific rate of gross photosynthesis	nmol O_2 cm^{-3} s^{-1}
PS(a)	Areal rate of gross photosynthesis	nmol O_2 cm^{-2} s^{-1}
J_{PS}	Areal rate of gross photosynthesis in energy terms	J m^{-2} s^{-1}
$J_{H\uparrow}$	Upward heat flux	J m^{-2} s^{-1}
$J_{H\downarrow}$	Downward heat flux	J m^{-2} s^{-1}
J_H	$J_{H\uparrow} - J_{H\downarrow}$	J m^{-2} s^{-1}
$E_d(\lambda)$	Downwelling photon irradiance	Counts nm^{-1}
$E_0(\lambda)$	Spectral scalar irradiance	% of $E_d(\lambda)$
$E_0(z)$	Local scalar irradiance availability	µmol photons m^{-2} s^{-1}
J_{IN}	Incident light energy	J m^{-2} s^{-1}
J_{ABS}	Absorbed light energy	J m^{-2} s^{-1}
R	Irradiance reflectance	
K_0	Diffuse attenuation coefficient of PAR	mm^{-1}
$K_0(\lambda)$	Spectral attenuation coefficient	mm^{-1}

biofilms, respectively. This indicates that by migration, the phototrophic community can apparently sustain similar energy conservation efficiencies, while avoiding the detrimental effects of excessive light when situated near the surface.

The vertical stratification of relative photosynthetic efficiencies (**Figure 6**) can either be ascribed to (i) a higher density of biomass contributing to photosynthesis, or (ii) an overall higher efficiency caused by higher cell specific pigment content and/or higher absorption cross section, in that area (Iglesias-Prieto and Trench, 1994, 1997; Falkowski and Raven, 2007; Al-Najjar et al., 2010). However, in our measurements we found differences in the vertical positions of the peaks of relative photosynthetic efficiency depending on light acclimation. At the cellular level, regulation of the pigment density and the absorption cross section of antennae pigments occurs on a longer time scale than the acclimation time used in these experiments, although the formation of zeaxanthin from β-carotene is a short term photoprotective mechanism (Falkowski and Raven, 2007). Given the time scale, the difference in vertical position of the peaks in relative photosynthetic efficiencies, can thus primarily be ascribed to migration.

In a fluctuating light environment, phototrophs can modulate light exposure/harvesting either by regulating pigment densities or by moving to a different light environment. For this mechanism to be energetically successful, the cost of motility must present an advantage compared to employment of regulation of light harvesting or photoprotective pigments. The cost of motility was estimated for *Oscillatoria* to be 0.2–5% of the energy generated by oxidative phosphorylation (Halfen and Castenholz, 1971). This is a relatively low cost considering that in a dense microbial system, where oxygenic phototrophs not only have to cope with alternating light environments but also steep and dynamic chemical gradients of e.g., pH and sulfide. Motility may thus be an important trait for phototrophs in microbial mats enabling rapid optimization of their light exposure and chemical microenvironment. Migration of cyanobacterial populations can also mitigate effects of continuous sedimentation and overgrowth by other microbes (Whale and Walsby, 1984).

Previously, photosynthetic quantum efficiencies in microbial mats have been calculated by applying a model that estimates the local quantity of absorbed light, which is then correlated to the local rates of gross photosynthesis (Al-Najjar et al., 2010). However, this model assumes a homogenous distribution of light absorption (i.e., biomass), which makes the application of such a model problematic in a motile community exhibiting photomovement. Calculations using the model of Al-Najjar et al. (2010) on our data showed apparent photosynthetic quantum efficiencies, about 2-fold higher than the theoretical maximum of 0.125 (i.e., 8 photons needed to produce 1 O_2 molecule). We speculate that the presence of a black ferrous sulfide layer in close proximity to the phototrophs also interfered with such estimations of the local density of absorbed light. However, the distribution of sand particles, organic matter and photosynthetic biomass was not further quantified, and a correction for this possible artifact was not attempted. Therefore, we estimated relative quantum efficiencies of photosynthesis by relating the depth specific gross photosynthesis rates to the scalar irradiance incident to that point following the approach of Lassen et al. (1992), who also found that the position of maximum quantum efficiencies changed with light exposure. The relative quantum efficiencies estimated in our mat samples were, however, up to three times higher than values reported by Lassen et al. (1992) for a less compacted microbial mat.

The photosynthetic efficiency depends on photo-pigmentation and other biotic/abiotic substances contributing to light absorption (Al-Najjar et al., 2012) but also on complex interplay between cyanobacteria and sulfur oxidizers (Klatt et al., 2016). Thus, the microscale 3D structure of the microbial mat will have an influence on the light availability and the energy balance of the system, where more open systems will display larger photic zones and different responses to changes in light environment as compared to more compacted systems

(Lichtenberg et al., 2017). How such microscale canopy-like effects in microbial mats are affected by the presence of much higher densities of abiotic matter in comparison to e.g., plant canopies remain to be studied in more detail.

CONCLUSION

We conclude that cyanobacteria can sustain high relative photosynthetic efficiencies by vertical migration in response to shifting light conditions, thereby optimizing the overall capacity of light absorption and photosynthetic activity against a backdrop of dynamic chemical gradients of O_2, pH and sulfide. This was evident from the overall photosynthetic energy conservation efficiency that did not change with light acclimation but showed vertical differences in the distribution of maximum relative photosynthetic efficiency. Further studies could investigate how distribution and efficiency of gross photosynthesis respond to changing light environment in microbial mats with vertically fixed populations of phototrophs in different depth horizons, e.g., by applying a motility inhibitor (Cartaxana et al., 2016a). In very compact systems such as the mats studied here it is, however, difficult to resolve local differences due to the spatial resolution of the microsensors and methodology to non-invasively monitor biomass distributions. In less compacted systems (e.g., mats like studied by Wieland and Kühl, 2000; Saenger et al., 2006; Lichtenberg et al., 2017) with more open structures and thereby less steep gradients of the physico-chemical parameters, local differences in energy deposition would be easier to describe in more detail.

Our study adds novel insight to the regulation of photosynthesis in compacted microbial mats and biofilms. In terms of energy conservation and photosynthetic efficiency, such systems are often regarded less efficient due to their more or less flat topography (e.g., Al-Najjar et al., 2012). However, there is increasing evidence that microstructural changes can modulate light harvesting and photosynthesis in dense photosynthetic biofilms and tissues, and that such systems can exhibit canopy-like properties at a microscale, where a more open microstructure and/or modulation of the scattering and lateral distribution of incident light seems to govern higher photosynthetic efficiency (e.g., Wangpraseurt et al., 2014; Lichtenberg et al., 2016, 2017; Lyndby et al., 2016). In the present study, we show that reorganization of the phototrophs via migration is yet another functional trait that helps optimize overall light harvesting and photosynthesis in biofilms and microbial mats.

DATA AVAILABILITY STATEMENT

The datasets generated for this study are available on request to the corresponding author.

AUTHOR CONTRIBUTIONS

ML, PC, and MK designed the experiments and analyzed the data. ML and PC performed the experiments. ML wrote the manuscript with editorial input from PC and MK.

FUNDING

This study was supported by grants from the Independent Research Fund Denmark (DFF-1323-00065B and DFF- 8021-00308B) (MK). PC acknowledges support from FCT/MCTES through CESAM (UIDB/50017/2020+UIDP/50017/2020).

ACKNOWLEDGMENTS

We thank Lars Rickelt for construction of scalar irradiance microprobes, and Sofie Jakobsen for excellent technical assistance. The members of the Microenvironmental Research Group provided useful feedback, help and suggestions during the experimental and analysis part of this study. Parts of this manuscript were included in the Ph.D. thesis of ML (Lichtenberg, 2017).

REFERENCES

Al-Najjar, M. A., de Beer, D., Kühl, M., and Polerecky, L. (2012). Light utilization efficiency in photosynthetic microbial mats. *Environ. Microbiol.* 14, 982–992. doi: 10.1111/j.1462-2920.2011.02676.x

Al-Najjar, M. A. A., de Beer, D., Jørgensen, B. B., Kühl, M., and Polerecky, L. (2010). Conversion and conservation of light energy in a photosynthetic microbial mat ecosystem. *ISME J.* 4, 440–449. doi: 10.1038/ismej.2009.121

Bebout, B. M., and Garcia-Pichel, F. (1995). UV B-induced vertical migrations of cyanobacteria in a microbial mat. *Appl. Environ. Microb.* 61, 4215–4222.

Bhaya, D. (2004). Light matters: phototaxis and signal transduction in unicellular cyanobacteria. *Mol. Microbiol.* 53, 745–754. doi: 10.1111/j.1365-2958.2004.04160.x

Brodersen, K. E., Lichtenberg, M., Ralph, P. J., Kühl, M., and Wangpraseurt, D. (2014). Radiative energy budget reveals high photosynthetic efficiency in symbiont-bearing corals. *J. R. Soc. Interf.* 11:20130997. doi: 10.1098/rsif.2013.0997

Burns, N. M., and Rosa, F. (1980). *In situ* measurement of the settling velocity of organic carbon particles and 10 species of phytoplankton. *Limnol. Oceanogr.* 25, 855–864.

Cartaxana, P., Cruz, S., Gameiro, C., and Kühl, M. (2016a). Regulation of intertidal microphytobenthos photosynthesis over a diel emersion period is strongly affected by diatom migration patterns. *Front. Microbiol.* 7:872. doi: 10.3389/fmicb.2016.00872

Cartaxana, P., Ribeiro, L., Goessling, J. W. L., Cruz, S., and Kühl, M. (2016b). Light and O2 microenvironments in two contrasting diatom-dominated coastal sediments. *Mar. Ecol. Prog. Ser.* 545, 35–47.

Coelho, H., Vieira, S., and Serôdio, J. (2011). Endogenous versus environmental control of vertical migration by intertidal benthic microalgae. *Eur. J. Phycol.* 46, 271–281.

De Beer, D., and Stoodley, P. (2013). "Microbial biofilms," in *The Prokaryotes - Applied Bacteriology and Biotechnology*, eds E. Rosenberg, E. DeLong, E. Stackebrandt, S. Lory, and F. Thompson (Berlin: Springer-Verlag), 343–372.

de Wit, R., and van Gemerden, H. (1987). Oxidation of sulfide to thiosulfate by *Microcoleus chtonoplastes*. *FEMS Microbiol. Ecol.* 45, 7–13.

Dillon, J. G., Miller, S., Bebout, B., Hullar, M., Pinel, N., and Stahl, D. A. (2009). Spatial and temporal variability in a stratified hypersaline microbial mat community. *FEMS Microbiol. Ecol.* 68, 46–58. doi: 10.1111/j.1574-6941.2009.00647.x

Falkowski, P., and Raven, J. A. (2007). *Aquatic Photosynthesis*, 2nd Edn, Princeton: Princeton University Press.

Fourcans, A., de Oteyza, T. G., Wieland, A., Solé, A., Diestra, E., van Bleijswijk, J., et al. (2004). Characterization of functional bacterial groups in a hypersaline microbial mat community (Salins-de-Giraud, Camargue, France). *FEMS Microbiol. Ecol.* 51, 55–70. doi: 10.1016/j.femsec.2004.07.012

Frigaard, N. U., Takaichi, S., Hirota, M., Shimada, K., and Matsuura, K. (1997). Quinones in chlorosomes of green sulfur bacteria and their role in the redox-dependent fluorescence studied in chlorosome-like bacteriochlorophyll c aggregates. *Arch. Microbiol.* 167, 343–349.

Glagoleva, T. N., Glagolev, A. N., Gusev, M. V., and Nikitina, K. A. (1980). Protonmotive force supports gliding in cyanobacteria. *FEBS Lett.* 117, 49–53.

Gorton, H. L., Williams, W. E., and Vogelmann, T. C. (1999). Chloroplast movement in *Alocasia macrorrhiza*. *Physiol. Plant.* 106, 421–428.

Gupta, S., and Agrawal, S. C. (2007). Survival and motility of diatoms *Navicula grimmei* and *Nitzschia palea* affected by some physical and chemical factors. *Folia Microbiol.* 52, 127–134. doi: 10.1007/BF02932151

Häder, D. P. (1987). "Photomovement," in *The Cyanobacteria*, ed. P. Fay (Amsterdam: Elsevier Science Publishers), 325–345.

Halfen, L. N., and Castenholz, R. W. (1971). Energy expenditure for gliding motility in a blue-green alga. *J. Phycol.* 7, 258–260.

Hoiczyk, E. (2000). Gliding motility in cyanobacteria: observations and possible explanations. *Arch. Microbiol.* 174, 11–17. doi: 10.1007/s002030000187

Iglesias-Prieto, R., and Trench, R. K. (1994). Acclimation and adaptation to irradiance in symbiotic dinoflagellates. Responses of the photosynthetic unit to changes in photon flux density. *Mar. Ecol. Prog. Ser.* 113, 163–175.

Iglesias-Prieto, R., and Trench, R. K. (1997). Acclimation and adaptation to irradiance in symbiotic dinoflagellates. II. Response of chlorophyll-protein complexes to different photon-flux densities. *Mar. Biol.* 130, 23–33.

Jekely, G. (2009). Evolution of phototaxis. *Philos. T. R. Soc. B* 364, 2795–2808.

Jensen, J., and Revsbech, N. P. (1989). Photosynthesis and respiration of a diatom biofilm cultured in a new gradient growth chamber. *FEMS Microbiol. Ecol.* 5, 29–38.

Jimenez, I. M., Kühl, M., Larkum, A. W. D., and Ralph, P. J. (2008). Heat budget and thermal microenvironment of shallow-water corals: do massive corals get warmer than branching corals? *Limnol. Oceanogr.* 53, 1548–1561.

Jørgensen, B. B. (1982). Ecology of the bacteria of the sulfur cycle with special reference to anoxic oxic interface environments. *Philos. T. R. Soc. B* 298, 543–561. doi: 10.1098/rstb.1982.0096

Jørgensen, B. B., and Revsbech, N. P. (1983). Colorless sulfur bacteria, *Beggiatoa spp. and Thiovulum spp. in O*2 and H2S microgradients. *Appl. Environ. Microb.* 45, 1261–1270.

Kamp, A., Roy, H., and Schulz-Vogt, H. N. (2008). Video-supported analysis of *Beggiatoa* filament growth, breakage, and movement. *Microb. Ecol.* 56, 484–491. doi: 10.1007/s00248-008-9367-x

Klatt, J. M., Meyer, S., Häusler, S., Macalady, J. L., de Beer, D., and Polerecky, L. (2016). Structure and function of natural sulphide-oxidizing microbial mats under dynamic input of light and chemical energy. *ISME J.* 10, 921–933. doi: 10.1038/ismej.2015.167

Kress, E., and Jahns, P. (2017). The dynamics of energy dissipation and xanthophyll conversion in *Arabidopsis* indicate an indirect photoprotective role of zeaxanthin in slowly inducible and relaxing components of non-photochemical quenching of excitation energy. *Front. Plant Sci.* 8:2094. doi: 10.3389/fmicb.2016.002094

Kühl, M. (2005). Optical microsensors for analysis of microbial communities. *Environ. Microbiol.* 397, 166–199. doi: 10.1016/S0076-6879(05)97010-9

Kühl, M., and Fenchel, T. (2000). Bio-optical characteristics and the vertical distribution of photosynthetic pigments and photosynthesis in an artificial cyanobacterial mat. *Microb. Ecol.* 40, 94–103. doi: 10.1007/s002480000061

Kühl, M., Glud, R. N., Ploug, H., and Ramsing, N. B. (1996). Microenvironmental control of photosynthesis and photosynthesis-coupled respiration in an epilithic cyanobacterial biofilm. *J. Phycol.* 32, 799–812.

Kühl, M., and Jørgensen, B. B. (1994). The light-field of microbenthic communities - radiance distribution and microscale optics of sandy coastal sediments. *Limnol. Oceanogr.* 39, 1368–1398.

Kühl, M., Lassen, C., and Jørgensen, B. B. (1994). "Optical properties of microbial mats: Light measurements with fiber-optic microprobes," in *Microbial Mats*, eds L. Stal and P. Caumette (Berlin: Springer), 149–166.

Kühl, M., Lassen, C., and Revsbech, N. P. (1997). A simple light meter for measurements of PAR (400 to 700 nm) with fiber-optic microprobes: application for P vs E0(PAR) measurements in a microbial mat. *Aquat. Microb. Ecol.* 13, 197–207.

Kühl, M., Trampe, E., Mosshammer, M., Johnson, M., Larkum, A. W. D., Frigaard, N.-U., et al. (2020). Substantial near-infrared radiation-driven photosynthesis of chlorophyll *f*-containing cyanobacteria in a natural habitat. *eLife* 9:e50871. doi: 10.7554/eLife.50871

Lassen, C., Ploug, H., and Jørgensen, B. B. (1992). Microalgal photosynthesis and spectral scalar irradiance in coastal marine sediments of Limfjorden Denmark. *Limnol. Oceanogr.* 37, 760–772.

Laviale, M., Ezequiel, J., Pais, C., Cartaxana, P., and Serôdio, J. (2015). The "creme brulee" sampler: a new high-resolution method for the fast vertical sampling of intertidal fine sediments. *J. Exp. Mar. Biol. Ecol.* 468, 37–44.

Lichtenberg, M. (2017). *Microscale Canopy Interactions in Aquatic Phototrophs*. Ph.D. dissertation, University of Copenhagen.

Lichtenberg, M., Brodersen, K. E., and Kühl, M. (2017). Radiative energy budgets of phototrophic surface-associated microbial communities and their photosynthetic efficiency under diffuse and collimated light. *Front. Microbiol.* 8:452. doi: 10.3389/fmicb.2016.00452

Lichtenberg, M., Larkum, A. W. D., and Kühl, M. (2016). Photosynthetic acclimation of *Symbiodinium in hospite* depends on vertical position in the tissue of the scleractinian coral *Montastrea curta*. *Front. Microbiol.* 7:230. doi: 10.3389/fmicb.2016.00230

Lyndby, N. H., Kühl, M., and Wangpraseurt, D. (2016). Heat generation and light scattering of green fluorescent protein-like pigments in coral tissue. *Sci. Rep.* 6:26599. doi: 10.1038/srep26599

Müller, P., Li, X. P., and Niyogi, K. K. (2001). Non-photochemical quenching. A response to excess light energy. *Plant Physiol.* 125, 1558–1566. doi: 10.1104/pp.125.4.1558

Nelson, D. C., and Castenholz, R. W. (1981). Organic nutrition of *Beggiatoa sp*. *J. Bacteriol.* 147, 236–247.

Nielsen, M., Revsbech, N. P., and Kühl, M. (2015). Microsensor measurements of hydrogen gas dynamics in cyanobacterial microbial mats. *Front. Microbiol.* 6:726. doi: 10.3389/fmicb.2016.00726

Nymark, M., Valle, K. C., Brembu, T., Hancke, K., Winge, P., Andresen, K., et al. (2009). An integrated analysis of molecular acclimation to high light in the marine diatom *Phaeodactylum tricornutum*. *PLoS One* 4:e7743. doi: 10.1371/journal.pone.0007743

Ploug, H., Lassen, C., and Jørgensen, B. B. (1993). Action spectra of microalgal photosynthesis and depth distribution of spectral scalar irradiance in a coastal marine sediment of Limfjorden, Denmark. *FEMS Microbiol. Ecol.* 12, 69–78.

Preisler, A., de Beer, D., Lichtschlag, A., Lavik, G., Boetius, A., and Jorgensen, B. B. (2007). Biological and chemical sulfide oxidation in a *Beggiatoa* inhabited marine sediment. *ISME J.* 1, 341–353. doi: 10.1038/ismej.2007.50

Ramsing, N. B., and Prufert-Bebout, L. (1994). "Motility of *Microcoleus chthonoplastes* subjected to different light intensities quantified by digital image analysis," in *Microbial Mats*, eds L. J. Stal and P. Caumette (Berlin: Springer), 183–191.

Revsbech, N. P. (1989). An oxygen microsensor with a guard cathode. *Limnol. Oceanogr.* 34, 474–478.

Revsbech, N. P., and Jørgensen, B. B. (1983). Photosynthesis of benthic microflora measured with high spatial-resolution by the oxygen microprofile method - capabilities and limitations of the method. *Limnol. Oceanogr.* 28, 749–756.

Richardson, L. L., and Castenholz, R. W. (1987). Diel vertical movements of the cyanobacterium *Oscillatoria terebriformis* in a sulfide-rich hot spring microbial mat. *Appl. Environ. Microb.* 53, 2142–2150.

Rickelt, L., Lichtenberg, M., Trampe, E., and Kühl, M. (2016). Fiber-optic probes for small scale measurements of scalar irradiance. *Photochem. Photobiol.* 92, 331–342. doi: 10.1111/php.12560

Saenger, C., Miller, M., Smittenberg, R. H., and Sachs, J. P. (2006). A physico-chemical survey of inland lakes and saline ponds: Christmas Island (Kiritimati) and Washington (Teraina) Islands, Republic of Kiribati. *Saline Syst.* 2:8. doi: 10.1186/1746-1448-2-8

Sand-Jensen, K., Binzer, T., and Middelboe, A. L. (2007). Scaling of photosynthetic production of aquatic macrophytes - a review. *Oikos* 116, 280–294.

Serôdio, J., Coelho, H., Vieira, S., and Cruz, S. (2006). Microphytobenthos vertical migratory photoresponse as characterised by light-response curves of surface biomass. *Estuar. Coast. Shelf S* 68, 547–556.

Stal, L. J. (1995). Physiological ecology of cyanobacteria in microbial mats and other communities. *New Phytol.* 131, 1–32.

Stomp, M., Huisman, J., Stal, L. J., and Matthijs, H. C. (2007). Colorful niches of phototrophic microorganisms shaped by vibrations of the water molecule. *ISME J.* 1, 271–282. doi: 10.1038/ismej.2007.59

Tamulonis, C., Postma, M., and Kaandorp, J. (2011). Modeling filamentous cyanobacteria reveals the advantages of long and fast trichomes for optimizing light exposure. *PLoS One* 6:e22084. doi: 10.1371/journal.pone.00022084

Terashima, I., Ooeda, H., Fujita, T., and Oguchi, R. (2016). Light environment within a leaf. II. Progress in the past one-third century. *J. Plant Res.* 129, 353–363. doi: 10.1007/s10265-016-0808-1

Thauer, R. K., Jungermann, K., and Decker, K. (1977). Energy conservation in chemotrophic anaerobic bacteria. *Bacteriol. Rev.* 41, 100–180.

Trampe, E., and Kühl, M. (2016). Chlorophyll *f* distribution and dynamics in cyanobacterial beachrock biofilms. *J. Phycol.* 52, 990–996. doi: 10.1111/jpy.12450

van Gemerden, H. (1993). Microbial mats - a joint venture. *Mar. Geol.* 113, 3–25.

Vogelmann, T. C. (1993). Plant-tissue optics. *Annu. Rev. Plant. Phys.* 44, 231–251.

Wada, M., Kagawa, T., and Sato, Y. (2003). Chloroplast movement. *Annu. Rev. Plant. Biol.* 54, 455–468.

Wangpraseurt, D., Larkum, A. W. D., Franklin, J., Szabo, M., Ralph, P. J., and Kühl, M. (2014). Lateral light transfer ensures efficient resource distribution in symbiont-bearing corals. *J. Exp. Biol.* 217, 489–498. doi: 10.1242/jeb.091116

Wangpraseurt, D., Larkum, A. W. D., Ralph, P. J., and Kühl, M. (2012). Light gradients and optical microniches in coral tissues. *Front. Microbiol.* 3:316. doi: 10.3389/fmicb.2016.00316

Webb, W. L., Newton, M., and Starr, D. (1974). Carbon dioxide exchange of *Alnus rubra* - a mathematical model. *Oecologia* 17, 281–291. doi: 10.1007/BF00345747

Whale, G. F., and Walsby, A. E. (1984). Motility of the cyanobacterium *Microcoleus chthonoplastes* in mud. *Br. Phycol. J.* 19, 117–123.

Wieland, A., and Kühl, M. (2000). Irradiance and temperature regulation of oxygenic photosynthesis and O2 consumption in a hypersaline cyanobacterial mat (Solar Lake. Egypt). *Mar. Biol.* 137, 71–85.

Wieland, A., Kühl, M., McGowan, L., Fourcans, A., Duran, R., Caumette, P., et al. (2003). Microbial mats on the Orkney Islands revisited: microenvironment and microbial community composition. *Microb. Ecol.* 46, 371–390. doi: 10.1007/s00248-002-0108-2

Conflict of Interest: The authors declare that the research was conducted in the absence of any commercial or financial relationships that could be construed as a potential conflict of interest.